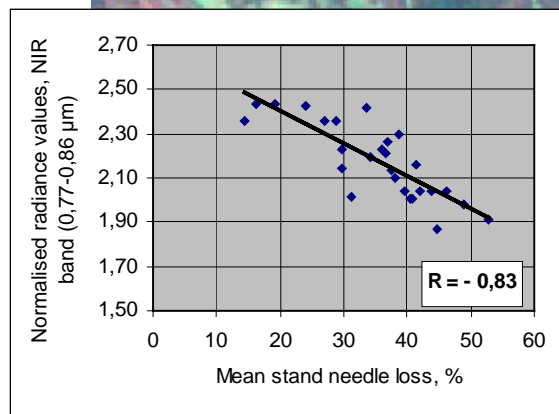
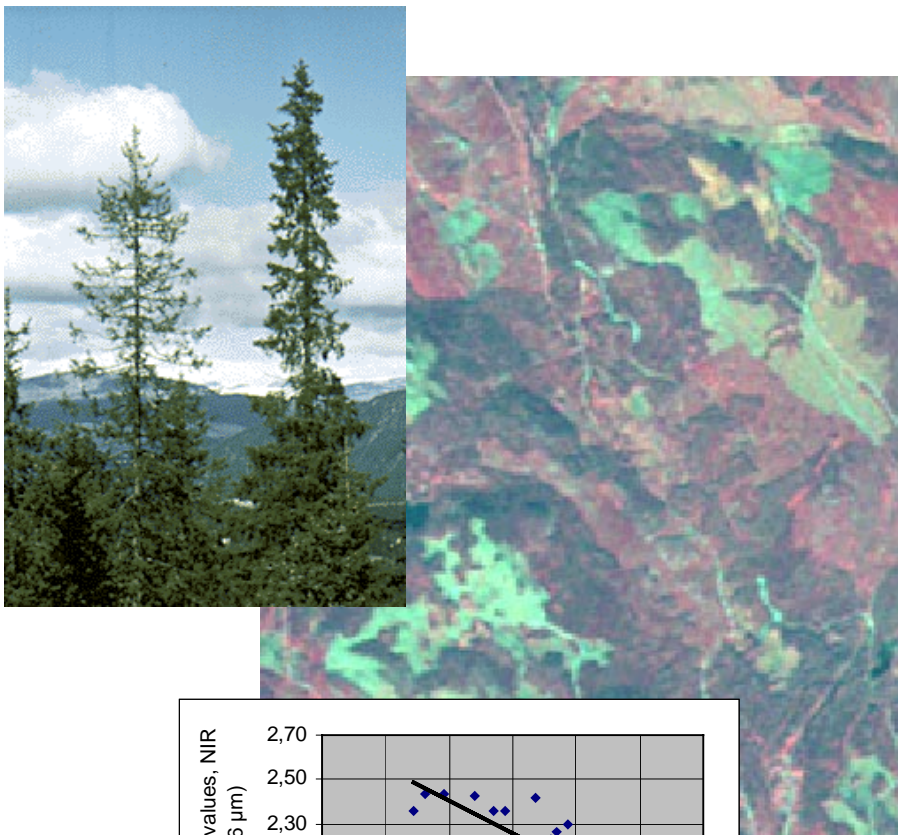




rapport

IVL Svenska Miljöinstitutet AB

Evaluation of IRS-1C LISS-3 satellite data for Norway spruce defoliation assessment



Helén Falkenström
B 1321
Stockholm, February 1999

Table of contents

Abstract.....	4
1. Introduction.....	5
1.1. Objectives	5
1.2. Satellite remote sensing and defoliation assessments	6
1.3. Factors influencing spectral effects of defoliation	7
1.3.1. Atmospheric effects	7
1.3.2. Forest stand parameters.....	7
1.3.3. Topography.....	7
1.4. IRS LISS-3.....	10
2. Material and methods.....	10
2.1. Study Area	10
2.2. Reference data.....	12
2.2.1. Interpretation of aerial photographs	12
2.2.2. Field survey.....	12
2.3. Satellite data preprocessing.....	12
2.3.1. Geometric transformation	12
2.3.2. Conversion of digital numbers to physical units	12
2.3.3. Correction for atmospheric effects.....	13
2.3.4. Extraction of radiance values	14
2.4. Normalisation of satellite data	14
2.4.1. Normalisation for topography	14
2.4.2. Normalisation for species composition	15
2.5. Correlation between spruce defoliation and LISS-3 data.....	15
2.6. Defoliation assessment algorithm and verification	15
3. Results and discussion	16
3.1. Normalisation of satellite data	16
3.1.1. Normalisation for topography	16
3.1.2. Normalisation for species composition	17
3.2. Correlation between spruce defoliation and LISS-3 data.....	18
3.3. Defoliation assessment algorithm and verification	19
3.4. IRS LISS-3 versus Landsat TM	20
3.5. Error sources	20
3.5.3. Correction for topography.....	21
3.5.4. Errors in reference data	21
3.5.5. Radiometric correction.....	21
4. Conclusion	22
References.....	23

Abstract

Satellite based remote sensing supported by air photo and field surveys, provide a means to area covering forest health assessment on a regional scale. Landsat TM data has been extensively used in studies of spruce and fir defoliation in Europe and North America. The temporal coverage of Landsat TM in combination with cloudiness however restrict the availability of data. In this study the LISS-3 sensor onboard the Indian Resource Satellite, IRS-1C, was evaluated for defoliation assessments in Norway spruce (*Picea abies*) in the central part of Sweden. The near infrared wavelength band proved to be best correlated with mean stand defoliation. After normalisation of satellite data for topographic conditions, the correlation coefficient increased from $-0,19$ to $-0,83$. Normalising satellite data for species composition did not improve the results though. The correction coefficients involved in the procedure were originally developed for Landsat TM, and proved to be inadequate for the LISS-3 data set. A thorough examination of the effects of species composition on LISS-3 data is needed to yield better results. The correlation between observed defoliation in the verification stands and predicted (based on the inverse regression function between corrected NIR values and defoliation in reference stands) was $0,70$, despite a very limited range of defoliation in the verification set. IRS-1C LISS-3 is fully comparable to Landsat TM for spruce defoliation studies, although the results would probably not be significantly improved.

1. Introduction

The issue of forest damage and decline attracted attention in the early 1980s when one of the economically most important coniferous species, Norway spruce (*Picea abies*), exhibited severe damage on a large scale in central Europe. In Sweden annual field surveys of forest defoliation and discoloration was initiated in 1984. Defoliation levels have proved to vary considerably between different years and geographic locations. Since the debate started the average percent of spruce trees in Sweden with a severe defoliation have increased, although the levels have stabilised during the last years (Berghäll et al., 1995).

The debate on cause-effect mechanisms has been extensive. Reduced vitality is connected to both natural causes such as ageing, climatic stress and insect attacks, and human induced stress by air pollution and soil acidification associated with nutrient deficiencies (Hällgren, 1995; Nihlgård, 1996; Schulze, 1989). The importance of each factor is a matter of discussion. Recent research indicates that there is not one global explanation, but many, depending on each specific case. A widely supported theory stress that tree vitality seldom is attributed to one single cause, but a consequence of the concise effect of a combination of stress factors (Nihlgård, 1996). Nevertheless, irrespective of cause there is a need for objective tools for area covering monitoring of short- and long-term changes in forest vitality.

Spaceborne techniques provide a means to assess defoliation on a regional scale and obtain area covering output instead of statistically based. Whereas defoliation in field surveys and aerial photography interpretation is estimated on single trees, assessments using satellite data concern the mean defoliation of a forest stand or a pixel. The spatial resolution of satellite data makes the radiance registered by the sensor in each pixel to be an integrated spectral response from the canopy and background reflectance. Factors such as structure of the canopy, species composition and topography thus tend to affect the assessments and needs to be corrected for.

The Landsat Thematic Mapper sensor, TM, has a resolution of 30 m and has been extensively used for studies of the earth in many disciplines. A problem, though, is the temporal coverage of the satellite data in combination with the fact that acquisitions frequently are affected by clouds. The time between two Landsat TM acquisitions is in Sweden 8 days. This means that during the vegetation season, end of May to the end of August, merely about ten acquisitions take place. Due to the mid latitude weather systems finding cloud free data is difficult. However, several new remote sensing satellites are on their way to be launched and with more satellites in orbit the possibility to encounter a cloud free scene from the time of ones interest will increase.

The Indian remote sensing satellite IRS-1C was launched in December 1995, and its twin satellite IRS-1D in September 1997. They carry a multispectral sensor, LISS-3 with a resolution of 23.5 m, a pancromatic camera with a 5.8 m resolution and a wide field sensor having a resolution of 188 m. The LISS-3 sensor is comparable with Landsat TM in both resolution and other technical aspects. If data from IRS LISS-3 could be used as an alternative to Landsat TM data, the chance of acquiring cloud free data would improve considerably and the remote sensing technique gain more interest.

1.1. Objectives

The overall aim of this study is to evaluate the performance of IRS-1C LISS-3 for assessing defoliation in Norway spruce (*Picea abies*). This includes:

1. To examine the correlation between mean stand defoliation and IRS-1C LISS-3 data.
2. To determine which LISS-3 band or combination of bands best discriminate among defoliation classes.
3. To compare the performance of IRS-1C LISS-3 and Landsat TM for defoliation studies

1.2. Satellite remote sensing and defoliation assessments

The possibility to use satellite-based remote sensing to assess defoliation has been thoroughly investigated by a number of authors. The majority of the studies concern Norway spruce (*Picea abies*) and Landsat TM data in the near and middle infrared regions of the electromagnetic spectra (e.g. Ekstrand, 1993; Lambert et al., 1995; Vogelmann, 1990). To a certain extent data from SPOT HRV has also been considered (Brockhaus et al.1992).

Significant correlations have been found between spruce defoliation and spectral reflectance registered by the satellite sensors. The near infrared band, NIR, is involved in all studies, but while some obtained best results with various kinds of band ratios (Häusler, 1991; Vogelmann and Rock, 1988; Vogelmann, 1990), others found the NIR band alone to be best correlated with defoliation (Brockhaus et al., 1992; Ekstrand, 1994; Heikkilä, 1998).

Spectral effects of spruce defoliation are reviewed in e.g. Ardö (1998) and Ekstrand (1993). Table 1 is a brief update of this information. The divergent effects of defoliation in the three spectral domains can be explained by the general characteristic of vegetation reflectance

In the visible domain leaf pigments absorb approximately 90 percent of the incoming radiation. The reflectance in the green region is slightly higher. Internal leaf structures give rise to a very high reflectance from green leaves in the NIR domain. The effect of an increased proportion of shadows and bark thus is much higher in the NIR domain than in the visible domain. The optical properties in the middle infrared domain, MIR, are dominated by water absorption. As the moisture content of the target decreases, the MIR reflectance increases (Swain and Davis, 1978).

Table 1: Changes of the spectral reflectance from a spruce stand attributed to various factors while the other factors are held constant. The stand is supposed to have a mean age above 70 years, be composed of 100% spruce, have a volume above 120 m³/ha, no defoliation and be situated in horizontal terrain.

	Visible	Near infrared	Middle infrared
Defoliation	slight decrease ¹ no effect ² increase ³	decrease ⁴ (less pronounced decrease) ⁵	increase ⁶ no effect ⁷
Pine and deciduous species	slight increase ⁸	increase ⁸	slight increase ⁸
Age	decrease ⁹	decrease ⁹	decrease ⁹

¹ A slight reduction in leaf cover generally increases the proportion of shadows and may cause a weak reflectance decrease (Koch et al., 1990).

² Loss of needles may also increase the spectral proportion of bark on the stem and branches, which have a higher reflectance than needles (Leckie et al., 1988; Rock et al., 1988) and thus may mask the shadowing effect. The occurrence of chlorosis (decreasing chlorophyll content) further increases the visible reflectance (Koch et al., 1990).

³ As the needle loss progress the exposure of bark is augmented, causing a reflectance increase (Leckie et al., 1988; Rock et al., 1988).

⁴ The high reflectance of vegetation is very sensitive to a decrease in biomass (Ekstrand, 1993; Koch et al., 1990; Rock et al., 1988). While some has attributed this to changes in the internal leaf structures (Rock et al., 1988), others explain it by increasing proportions of shadows and bark. (Koch et al., 1990). Bark and branches has a lower NIR reflectance than needles (Leckie et al., 1988).

⁵ When the canopy becomes very sparse the understory may be visible through bark and branches. A bright understory such as grass has been shown to result in higher canopy reflectance than a less reflecting understory (Colwell, 1974). Although it has not been shown in any defoliation studies, this may reduce the NIR decrease at severe defoliation.

⁶ A decrease in leaf biomass reduces the water absorption. The resulting increase in reflectance may be emphasised by an increased exposure of bark and background, which have a higher reflectance than conifer needles (Koch et al., 1990).

⁷ In some studies a weak, or no response at all were found (Ekstrand, 1993).

⁸ Both pine and deciduous species, particularly deciduous, have a higher reflectance than spruce (Kleman, 1986). Whereas the increase is weak in the visible and middle infrared domain, it is relatively strong in the near infrared band (Ekstrand, 1993).

⁹ Reflectance generally decreases with age (Kleman, 1986). This effect is most pronounced in the NIR and MIR domain (Ekstrand, 1993).

1.3. Factors influencing spectral effects of defoliation

The spectral response of light and moderate defoliation is subtle and the capability to detect defoliation using satellite and airborne data has proved to be very sensitive to atmospheric effects, variations in forest stand characteristics and terrain (e.g. Ekstrand, 1993; Leckie, 1987). In order to study defoliation these factors thus need to be addressed.

1.3.1. Atmospheric effects

Scattering and absorption by molecules and aerosols in the atmosphere affect all spaceborne data and there are different ways to handle the problem. Absolute correction requires data on physical and meteorological parameters as well as background reflectance values. The atmospheric effects are derived using a radiance transfer model (e.g. Kawata et al., 1988). Indirect corrections are based on assumed or field measured radiance from certain ground targets. By subtracting the radiance observed by the sensor with the known radiance, the path radiance is deduced. This approach neglects the atmospheric absorption and simply corrects for path radiance (Chavez, 1988).

A widely used indirect approach is dark object subtraction. Dark objects such as shadows and lakes are assumed to be completely, or nearly completely, black surfaces. Hence, the radiance registered at these targets is assumed to be an effect of path radiance. By subtracting the whole image with the radiance registered at the dark targets, the path radiance is considered eliminated. Each band needs subtraction with specific values since the scattering is wavelength dependent (Chavez, 1988). This approach assumes a horizontally uniform atmosphere, which is rarely the case. The aerosol and water content can vary significantly in space (Kaufman and Tanré, 1996). However, spatial information of these parameters is in most cases not available. In this study a dark object subtraction was applied since neither meteorological data nor background reflectance values were available.

1.3.2. Forest stand parameters

Reflectance values in both the visible, near- and middle infrared parts of the spectrum generally decrease with age, biomass, canopy closure, leaf area index and forest stand volume. These factors are usually positively correlated to each other. As the canopy closure reaches 100 percent the negative relation with reflectance ceases. Volume continues to increase with age but no further decrease in reflectance will occur due to the sensitivity of the remotely sensed signal to canopy closure (Franklin, 1986). The main reflectance change occurring with age (Table 1) is in fact caused by changes in canopy structure associated with age (and management practices) (Ekstrand, 1993).

Species composition has a large influence on the forest stand reflectance and the ability to assess defoliation (Ekstrand, 1994; Leckie, 1987; Wastenson et al., 1987). Ekstrand (1994) found that a component of 25 percent pine completely neutralises the spectral effect of a 10 percent needle loss. Similarly is the spectral effect from a deciduous component of 20 percent in the same magnitude as a 20 percent needle loss.

No standardised method to account for the effects of forest stand variations exists. In some investigation areas with homogeneous, monocultural and dense forest, it has not been considered necessary. In other studies, only areas with similar forest conditions have been selected for the study. Ekstrand (1994) studied the effect of pine and deciduous trees in Swedish spruce forest. Subtraction constants were empirically derived and multiplied with the percent of pine and deciduous content. The resulting value was then subtracted from the original satellite number. This approach was tested in the present study.

1.3.3. Topography

Topography affects the sensor-registered radiance in several ways. The irradiance received by the target varies with the cosine of the angle between the sunbeam and the surface normal, i.e. the incidence angle (Figure 1). The larger the incidence angle, the less the amount of radiation reaching the surface (Teillet et al., 1982). As the target receives less electromagnetic radiance, less electro-magnetic radiance is reflected, if all other factors are constant.

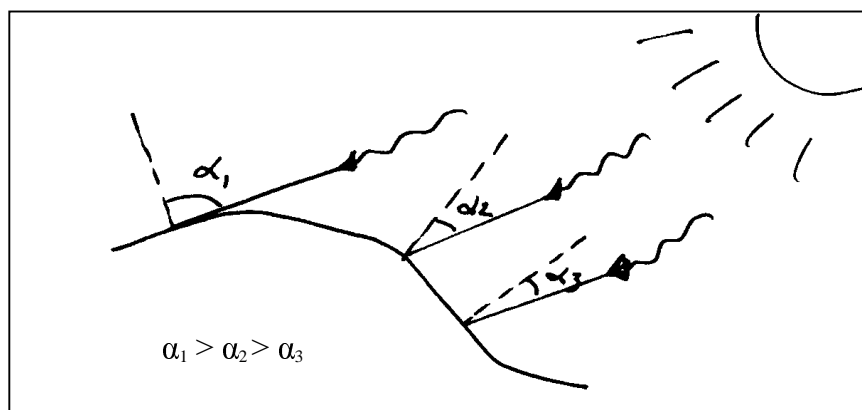


Figure 1: The incidence angle, α , is the angle between the sunbeam and the surface normal. A larger incidence angle means that less radiation reaches the surface.

Due to atmospheric scattering, the radiance received by the sensor is affected by the sun elevation as well. A lower sun elevation means a longer transportation for the sunbeam, and the effect of scattering is hence larger (Ekstrand, 1993). To some extent the target altitude also have an effect on the sensor-registered radiance). This is because the optical thickness of the atmosphere decreases with altitude and the optical thickness affects the scattering (Yugui, 1989).

The amount of radiance reflected by the target depends on the class-specific reflection in different directions. But the class-specific reflection may change with topography if the geometric structure within the class, e.g. a forest canopy, change (e.g. Kriebel, 1976). Different types of vegetation respond differently to direction and illumination effects (e.g. Thomson and Jones, 1990). A pine forest does for example not respond in the same way as a spruce forest. The relative importance of slope-aspect effects in forest reflectance is in fact not very well understood.

Several topographic correction models have been developed to remove the effects caused by terrain variations. However, so far no correction procedure has been published that is valid and adequate for all vegetation types. Three common methods are the Lambert cosine correction, the Minnaert correction and the C-correction (further described below). To work with band ratios instead of single bands, and in this way avoid the terrain effects, is another approach. It has been reported to be effective provided that the atmospheric path term is eliminated (Kowalik et al., 1983). Still another way to address the problem is to correct for the effects of topography together with the atmospheric effects in a radiance transfer model (e.g. Kawata et al., 1988).

Lambert cosine correction: The Lambert cosine correction (Equation 1) assumes the target is a perfect diffuse reflector, i.e. that the reflectance is independent of viewing geometry. Hence, it only attempts to correct for illumination differences caused by surface orientation (Teillet et al., 1982). But very few surfaces are perfect diffuse reflectors (e.g. Lillesand and Kiefer, 1994).

$$L(\lambda)_{\text{corr}} = L(\lambda)_{\text{uncorr}} \cdot \cos(z) / \cos(i) \quad \text{Equation 1 (Teillet et al., 1982)}$$

$$\cos i = \cos(e) \cdot \cos(z) + \sin(e) \cdot \sin(z) \cdot \cos(\phi_s - \phi_n) \quad \text{Equation 2 (Smith et al., 1980)}$$

- $L(\lambda)_{\text{uncorr}}$ = spectral radiance measured by sensor ($\text{mWcm}^{-2}\text{sr}^{-1}\mu\text{m}^{-1}$)
- $L(\lambda)_{\text{corr}}$ = spectral radiance corrected for topography ($\text{mWcm}^{-2}\text{sr}^{-1}\mu\text{m}^{-1}$)
- i = incidence angle, the angle between surface normal and solar beam ($^\circ$)
- z = solar zenith angle ($^\circ$)
- e = slope of reference site ($^\circ$)
- ϕ_s = solar azimuth angle ($^\circ$)
- ϕ_n = slope aspect of reference site ($^\circ$)
- $\phi_s - \phi_n$ = 'relative azimuth' ($^\circ$)

When sun elevation is low and northern slopes are in shadow no radiance would occur according to the Lambertian assumption. This is not true since diffuse sky irradiance will always reach the surface during daytime. According to Deering et al. (1994) sky irradiance may contribute to up to 15 percent of the total near infrared irradiance, and in the visible bands to as much as 25 percent.

The cosine correction usually underestimates reflectance on sun-facing slopes and overestimate reflectance on slopes facing away from the sun. Except for situations with high sun elevations, the cosine correction has proved to be inadequate for forest vegetation (e.g. Teillet et al., 1982; Smith et al., 1980).

Minnaert correction: The Minnaert correction (Equation 3) is a variation of the cosine correction and is based on the Minnaert law (Minnaert, 1941). A constant k , which is no real constant since it is wavelength and surface dependent, is introduced to simulate the non-Lambertian behaviour of the earth surface. The Minnaert constant is a measure of how close a surface is to the ideal reflector, for which $k=1$ (Smith et al., 1980).

$$L(\lambda)_{\text{corr}} = L(\lambda)_{\text{uncorr}} \cdot \cos(e) / [\cos^k(i) \cdot \cos^k(e)]$$

Equation 3 (Smith et al., 1980)

k = Minnaert constant

C-correction: Teillet et al. (1982) examined a modified version of the cosine correction where a linear relation between radiance and cosine of the incidence angle is still assumed. To avoid over correction they introduced a band specific constant derived from regression functions between radiance and cosine of the incidence angle. The constant is called C and is calculated by dividing the offset of the regression line with its slope.

$$L(\lambda)_{\text{corr}} = L(\lambda)_{\text{uncorr}} \cdot [\cos(z) + C] / [\cos(i) + C]$$

Equation 4 (Teillet et al., 1982)

$C = a/m$

C = C-constant
 a = offset of regression line
 b = slope of regression line

Meyer et al. (1993) tested the three correction models described above on TM forest images. The Minnaert and c-correction both produced better results than the cosine correction. Best result was achieved with the c-correction, but some degree of over- and underestimation remained also after the c-correction.

Ekstrand (1996) found a non-linear relation between radiance and cosine of the incidence angle when studying terrain effects on spruce forests in Sweden. He tested the Minnaert correction with previously developed constants, but the method was ineffective when a single constant for each spectral band was used. When new constants were derived, however, and they were allowed to vary with the cosine of the incidence angle, the corrections proved adequate. For the near infrared channel residuals of $0,02 \text{ mWcm}^{-2}\text{sr}^{-1}\mu\text{m}^{-1}$ remained after correction.

The residual effects that remains after correction have generally been attributed to a neglecting of the diffusive illumination and poor digital terrain models (Civco, 1989). However, as pointed out by Ekstrand (1993), there are gaps in the information about e.g. the diffuse sky irradiance, the class specific reflection in different directions and changes in geometric canopy structure.

In this study the semi-empirical approach developed by Ekstrand (1996) for spruce forest and Landsat TM data was applied.

1.4. IRS LISS-3

The orbital characteristics of IRS-1C/1D are listed and compared to the Landsat satellites in Table 2.

The Linear Imaging Self-Scanning Sensor 3, LISS-3, is a multispectral scanner working in pushbroom mode. It employs a linear array of 6000 CCD:s for each band except for the SWIR band, which uses a 2100 element linear CCD array. Sensor characteristics for LISS-3 and the Thematic Mapper sensor, TM, are given in Table 3.

LISS-3 provides data in four spectral bands, the green, red, near infrared and middle infrared part of the spectra (Table 4). The spectral bands are titled 2, 3, 4 and 5. More details of the IRS-1C and 1D spacecrafts and their camera systems are given by Kalyanaraman et al. (1995).

Table 2: Orbital characteristics of IRS-1C and Landsat 4 and 5 (modified from Kalyanaraman et al., 1995).

	IRS-1C	Landsat 4, 5
Orbit type	Near-polar sun-synchronous	Near-polar sun-synchronous
Altitude	817 km	705 km
Inclination	98.69 °	98.2 °
Time of equator crossing	10.30 A.M. local sun time	9.45 A.M. local sun time
Distance between adjacent traces	117,5 km	172 km

Table 3: Sensor characteristics for LISS-3 and TM (modified from Kalyanaraman, Rajangam and Rattan, 1995).

	LISS-3	TM
Geometric resolution	23.6 m (70.8 m ¹)	30 m (120 m ²)
Radiometric resolution	7 bits	8 bits
Scanner type	Along track	Across track
Swath width	142 km for bands 2, 3, 4 148 km for band 5	185 km
Repetivity	24 days	16

(¹ Middle infrared channel, ² Thermal infrared)

Table 4: The spectral bandwidths of LISS-3 are slightly different from those of TM.

	LISS-3	TM
Band 1, blue	-	0.45-0.52 μm
Band 2, green	0.52-0.59 μm	0.52-0.60 μm
Band 3, red	0.62-0.68 μm	0.63-0.69 μm
Band 4, nir	0.77-0.86 μm	0.76-0.90 μm
Band 5, mir	1.55-1.70 μm	1.55-1.75 μm
Band 6, thermal	-	2.08-2.35 μm

2. Material and methods

2.1. Study Area

The study area is located in the county of Västernorrland in the boreal region of Sweden, see Figure 2. Productive forestland constitutes 74 percent of the land in Västernorrland. This makes it one of Sweden's most forest dominated regions. The industrialisation of the region had much to owe the forest trade, which still is very important for the economy in the area.

The bedrock is dominated by sedimentary gneiss with patches of pegmatite and granite. On top of this sandy or silty till is found sometimes only a thin layer. Mean annual temperature is 3,4 °C and mean annual precipitation is 627 mm. The terrain is hilly with altitudes ranging from 100-400 m and slopes reaching 25 degrees.

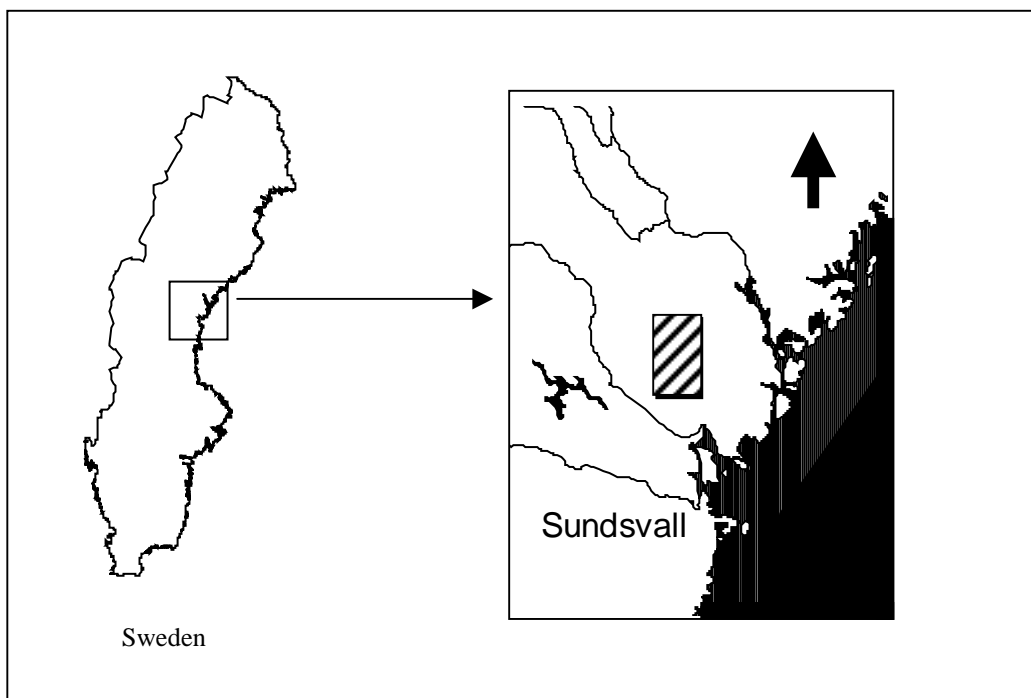


Figure 2: Location of study area.

Norway spruce (*Picea abies*) is the major species of the forest stands (Figure 3). It is mixed with minor components of Scots pine (*Pinus sylvestris*), birch (*Betula verrucosa*, *B. pubescens*) and aspen (*Populus tremula*). Stands entirely composed of Scots pine are also found, as well as parcels with deciduous trees, particularly around wetlands.

The density of the forest stands in northern Sweden is generally lower than in the southern part and on the European continent. Furthermore are defoliation levels often higher than in the south of Sweden, which to a large extent can be attributed to the harsh climate. Data from the National Forest Inventory over Västernorrland and neighbouring counties reveal an average defoliation of 26 percent for the years 1989-1993.

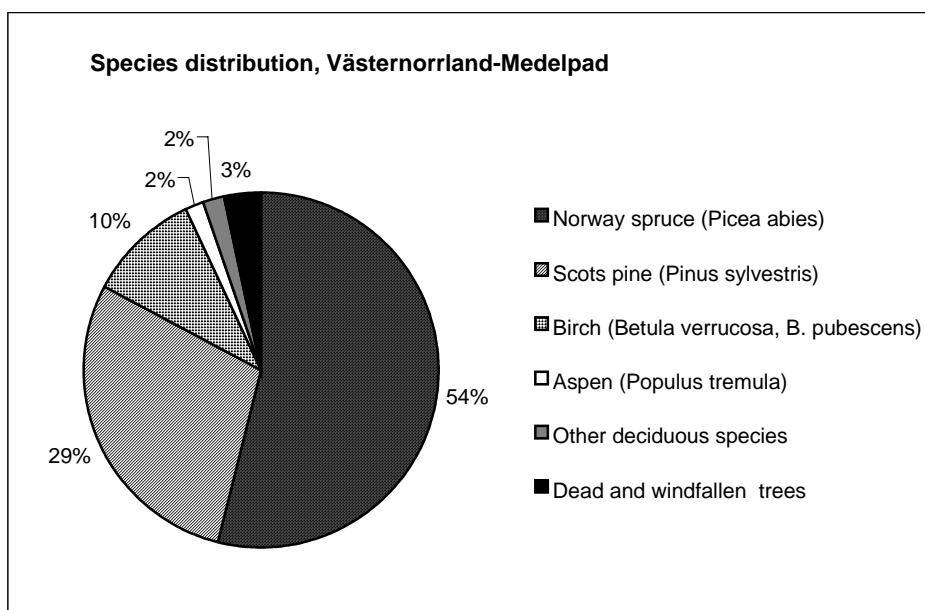


Figure 3: Average species distribution in the county of the study area (based on data from the National Forest Inventory, 1998).

2.2. Reference data

2.2.1. Interpretation of aerial photographs

Parallel to the satellite data acquisition an air photo survey was performed. A land strip covered by the satellite scene was photographed on the 22 September 1997 with colour infrared, CIR film. From the resulting CIR photographs on the scale of 1:6000, 50 reference sites with an approximate size of one hectare were selected. Only spruce dominated stands older than 70 years, and with fairly homogeneous canopy, was considered. In order to facilitate the subsequent delineation of the sites in the satellite image, sites close to objects that could easily be distinguished in the image were selected, such as a younger stand, small forest gap, a road or cutting.

Defoliation and species composition of the reference sites were interpreted manually from the CIR photographs using a stereoscope. All clearly visible trees were assessed in respect to species (spruce, pine or deciduous) and defoliation level. Defoliation was estimated in 20 percent classes (0-20, 21-40, 41-60, 61-80 and 81-100 percent). Mean spruce needle loss for each stand was calculated by summing the number of trees in each class and multiplying with the class midpoint. The sums from the five classes were averaged resulting in a mean needle loss for the site.

2.2.2. Field survey

To obtain reference data for the air photo interpretation, fully 200 trees were field assessed at the time of satellite registration. Needle loss was assessed in 5 percent classes according to the methods of the National Forest Inventory (Wulff and Löfberg 1998). The air photo based defoliation was thus calibrated to the annual defoliation assessments of the National Forest Inventory.

Data on mean slope and aspect of the reference sites was obtained during a subsequent field visit supported by air photo interpretation. During the field visit age and homogeneity of the stands were also surveyed to verify the stratification of the reference sites selection.

2.3. Satellite data preprocessing

An IRS-1C LISS-3 scene acquired on 25 September 1997 (path 26, row 22) at the Neustrelitz groundstation in Germany was obtained from the European distributor EuroMap. The sun elevation was 26,5 degrees and the solar azimuth 177 degrees. Data was purchased path oriented, i.e. geometrically corrected to the orientation of the ground track. The pixel size was 25 m and the pixel numbers stretched to eight bit values.

The Erdas Imagine software was used for all image processing.

2.3.1. Geometric transformation

To transform the IRS data to a map grid, an image to image transformation was performed using a Landsat TM scene corrected to the Swedish national grid by SSC Satellitbild. 25 evenly distributed Ground Control Points, GCP: s, were employed in a first order polynomial transformation. Total Root Mean Square Error, RMSE, was 10,3 m, i.e. less than ½ pixel. Maximum RMSE for a single GCP was 15 m. Cubic Convolution was used for the resampling process and the pixel size was preserved at 25 m.

2.3.2. Conversion of digital numbers to physical units

The digital numbers, DN_s, registered by the sensor were converted to satellite radiance using calibration coefficients supplied by the data contractor (Table 5) and Equation 5.

$$L(\lambda) = \frac{[L(\lambda)_{\max} - L(\lambda)_{\min}]}{DN_{\max}} \cdot DN(\lambda) + L(\lambda)_{\min} \quad \text{Equation 5 (Markham and Barker, 1987)}$$

- $L(\lambda)$ = spectral radiance ($\text{mW cm}^{-2} \text{sr}^{-1} \mu\text{m}^{-1}$)
- $L(\lambda)_{\max}$ = maximum spectral radiance ($\text{mW cm}^{-2} \text{sr}^{-1} \mu\text{m}^{-1}$) registered by the sensor
- $L(\lambda)_{\min}$ = minimum spectral radiance ($\text{mW cm}^{-2} \text{sr}^{-1} \mu\text{m}^{-1}$) registered by the sensor
- DN = digital number, absolute calibrated by the distributor
- DN_{\max} = maximum digital number

Table 5: Minimum and maximum spectral radiance registered by LISS-3 compared to corresponding values for TM. To be used in Equation 1. From Euro Map (LISS-3) and Markham and Barker, 1987 (TM).

Band	L(max) (mWcm ⁻² sr ⁻¹ μm ⁻¹)	L(min) (mWcm ⁻² sr ⁻¹ μm ⁻¹)
LISS-3, 2, green	14,45	1,76
TM 2, green	29,68	- 0,28
LISS-3, 3, red	17,03	1,54
TM 3, red	20,43	- 0,12
LISS-3, 4, nir	17,19	1,09
TM 4, nir	20,68	- 0,15
LISS-3, 5, mir	2,42	0
TM 5, mir	2,719	0,037

Data was generally expressed in radiance values. However, in some operations it was more feasible to express data in digital numbers (correction for species composition). The atmospheric correction even required reflectance values, Equation 6. Values of mean solar exoatmospheric irradiance for the different channels were calculated from Wolfe and Zissis (1989) (Table 6). For the earth-sun distance a table value from September 1996 was used (Astrophysical & Planetary Sciences University of Colorado <http://lyra.colorado.edu/sbo/astroinfo/hale-bopp/triangles.html>).

$$\rho(\lambda) = (L(\lambda) \cdot \pi \cdot d^2) / (\cos z E_{\text{sun}}(\lambda)) \quad \text{Equation 6 (Markham and Barker, 1987)}$$

- $\rho(\lambda)$ = reflectance (%)
- $L(\lambda)$ = spectral radiance (mW cm⁻² sr⁻¹ μm⁻¹)
- d = earth-sun distance (astronomical units)
- z = solar zenith angle (°)
- $E_{\text{sun}}(\lambda)$ = mean solar exoatmospheric irradiance, from Table 6 (mW cm⁻² μm⁻¹)

Table 6: Mean values of the solar exoatmospheric irradiance within the bands of LISS-3, calculated from Wolfe and Zissis (1989) and compared to corresponding values for TM (Markham and Barker, 1987).

	IRS-1C LISS-3	Landsat TM
Band 2, green	175,2 (0.52-0.59 μm)	182,9 (0.52-0.60 μm)
Band 3, red	151,4 (0.62-0.68 μm)	155,7 (0.63-0.69 μm)
Band 4, nir	107,4 (0.77-0.86 μm)	104,7 (0.76-0.90 μm)
Band 5, mir	22,3 (1.55-1.70 μm)	21,7 (1.55-1.75 μm)

2.3.3. Correction for atmospheric effects

In the absence of relevant background reflectance values and meteorological and atmospheric data, the correction for atmospheric effects was accomplished with a dark object subtraction.

Bukata et al. (1983) measured water spectral radiance in water with very small concentrations of suspended sediment and phytoplankton. In contrast to what is sometimes assumed, they discovered that even clear deep water reflects a small proportion of the visible light. For the green and red wavelength bands the reflectance found was 2,0 and 0,4 percent respectively.

Based on this information radiance values from 25 lakes were extracted and subtraction values were calculated and applied to each band (Equation 7, 8 and Table 7).

$$C_{\text{sub}} = L(\lambda) - L(\lambda)_0 \quad \text{Equation 7}$$

$$L(\lambda)_0 = (\rho(\lambda) \cos z E_{\text{sun}}(\lambda)) / (\pi d^2) \quad \text{Equation 8}$$

- C_{sub} = subtraction value ($\text{mW cm}^{-2} \text{sr}^{-1} \mu\text{m}^{-1}$)
 $L(\lambda)$ = radiance measured by sensor ($\text{mW cm}^{-2} \text{sr}^{-1} \mu\text{m}^{-1}$)
 $L(\lambda)_0$ = radiance reflected by target ($\text{mW cm}^{-2} \text{sr}^{-1} \mu\text{m}^{-1}$)
 $\rho(\lambda)$ = reflectance from dark lakes (%), from Bukata et al, 1983
 d = earth-sun distance (astronomical units)
 z = solar zenith angle ($^\circ$)
 $E_{\text{sun}}(\lambda)$ = mean solar exoatmospheric irradiance, ($\text{mW cm}^{-2} \mu\text{m}^{-1}$), from Table 6

Table 7: Subtraction values calculated from Equation 3 and 4.

	Subtraction value ($\text{mWcm}^{-2}\text{sr}^{-1}\mu\text{m}^{-1}$)	Subtraction value (DN)
LISS-3, 2, green	2,88	23
LISS-3, 3, red	2,36	14
LISS-3, 4, NIR	1,73	10
LISS-3, 5, MIR	0,139	15

2.3.4. Extraction of radiance values

The reference sites were located and delineated in the satellite image by visual inspection. Border pixels were excluded from the analysis in order to avoid influence from spectrally divergent pixels nearby (see section 2.2.1.). From each site mean radiance for all spectral bands was extracted for further analysis.

2.4. Normalisation of satellite data

Based on the information from previous studies (Ekstrand, 1994; Leckie, 1987) a normalisation of radiance values for topography and species composition in the reference stands was assumed to be necessary.

2.4.1. Normalisation for topography

An empirical correction procedure developed by Ekstrand (1996) for spruce forest and TM data under Scandinavian conditions was applied to the data (Equation 9). The algorithm is a modification of the widely used Minnaert correction. The Minnaert constants derived for Norway spruce (Table 8) are here allowed to change with the cosine of the incidence angle in order to avoid the over and under estimations which otherwise affect the data (see section 1.3.3.).

The fact that the Minnaert constants in Table 8 originally were developed for Landsat TM, with slightly different bandwidths compared to LISS-3, was assumed to be of minor importance.

$$L(\lambda)_{\text{corr}} = L(\lambda) \cdot (\cos z / \cos i)^{r \cdot \cos i} \quad \text{Equation 9 (Ekstrand, 1996)}$$

- $L(\lambda)$ = spectral radiance measured by sensor ($\text{mWcm}^{-2}\text{sr}^{-1}\mu\text{m}^{-1}$)
 $L(\lambda)_{\text{corr}}$ = spectral radiance corrected for topography ($\text{mWcm}^{-2}\text{sr}^{-1}\mu\text{m}^{-1}$)
 z = solar zenith angle ($^\circ$)
 $\cos i$ = incidence angle, the angle between surface normal and solar beam ($^\circ$), see Equation 2.
 $r \cdot \cos i$ = Minnaert constant, for r , see table 9
 e = slope of reference site ($^\circ$)
 ϕ_s = solar azimuth angle ($^\circ$)
 ϕ_n = slope aspect of reference site ($^\circ$)
 $\phi_s - \phi_n$ = 'relative azimuth' ($^\circ$)

Table 8: Minnaert constants to be employed in Equation 9 (Ekstrand 1996).

Spectral band	Minnaert constant
LISS-3, 2, green	$0,34 \cdot \cos i$
LISS-3, 3, red	0,56 (relative azimuth 0-90°) 0,36 (relative azimuth 91-180°)
LISS-3,4, NIR	$1,04 \cdot \cos i$ (relative azimuth 0-60°) $0,97 \cdot \cos i$ (relative azimuth 61-180°)
LISS-3, 5, MIR	$0,94 \cdot \cos i$

2.4.2. Normalisation for species composition

Reference data was not sufficient for a thorough study of the spectral effect of a variation in species composition. Instead correction coefficients derived by Ekstrand (1994) were modified and used.

To obtain at least some information on the general radiometric level in the LISS-3 scene compared to the Landsat TM scene on which the correction coefficients previously had been used, DN values from the two data sets were compared. Five deciduous stands (100 percent) were also located in both data sets. Digital numbers for each of the spectral bands were extracted and the digital numbers for these sites, as well as all the reference sites, were plotted against corresponding deciduous components. The resulting regression lines were studied and correction coefficients were derived (see section 3.1.2).

Satellite data was finally normalised using the correction coefficients and data on species composition from the air photo survey (Equation 10).

$$DN_{\text{corr}}(\lambda) = DN(\lambda) - C_{p(\lambda)} P - C_{d(\lambda)} D \quad \text{Equation 10 (Ekstrand, 1996)}$$

$DN(\lambda)$ = digital number normalised for topography

$DN_{\text{corr}}(\lambda)$ = digital number, corrected for pine and deciduous species components

P = pine component (%)

D = deciduous species component (%)

$C_{p(\lambda)}$ = correction coefficient for the pine element

$C_{d(\lambda)}$ = correction coefficient for the deciduous species element

2.5. Correlation between spruce defoliation and LISS-3 data

Half of the reference sites were selected for use in the correlation analysis and remaining sites were left for evaluation. The selection was stratified in respect to defoliation levels in order to have a wide range of defoliation levels in both data sets.

The relationship between satellite data and defoliation was examined with regression analysis. Correlation coefficients between defoliation and single spectral bands, as well as a number of indices were calculated both for corrected and non-corrected data.

The correlation coefficient is a measure of the strength of the relationship between two sets of variables. The stronger the relation, the closer the correlation coefficient is to 1. Whether the relation is a matter of chance or not is described by the statistical significance. Significance at the 0,05 level for 30 observations requires a correlation coefficient of 0,306, and at the 0,01 level 0,432 (Hammond and McCullagh, 1978).

2.6. Defoliation assessment algorithm and verification

The regression equation yielding highest correlation between satellite data and defoliation was inverted and used as an assessment algorithm. The assessment algorithm was verified by regression analysis of observed versus predicted defoliation of the verification data set. Defoliation of the sites not used in the correlation analysis was predicted with the assessment algorithm and plotted against the levels observed in the air photo interpretation.

3. Results and discussion

Visual inspection of the image data revealed a systematic striping within the visible and middle infrared bands, most apparent against dark backgrounds such as lakes. In Fourier spectra the stripes were clearly seen as a narrow band from the upper left part of the spectra to the lower right side, indicating stripes stretching from north-east to south-west in the images, i.e. along the satellite track.

Striping effects in LISS-3 data have been reported from other authors as well. The origin of the striping is presumably an imbalance in the radiometric response of the CCD elements. Several destriping procedures exist. Although the pixel values by no means are raw; they have been subjected to calibration at the ground station as well as geometric correction, it was thought inappropriate to interfere with the digital numbers as the exact cause of the stripes were not known.

3.1. Normalisation of satellite data

3.1.1. Normalisation for topography

The normalisation procedure reduced the radiance registered from south facing slopes and increased the response from north facing slopes. The steeper the slope, the larger the correction.

The resulting change in the NIR channel ranged from a reduction of 10 DN (in a 17 ° SW slope) to an increase of 6 DN (in a 10 ° N slope). In the other channels the normalisation did not result in such large modifications of the values. The effect of shadows is larger in the NIR domain than in the visible and MIR domains due to the large difference in reflection by vegetation and shadows (Koch et al., 1990).

The result was evaluated by plotting the topographic residuals, i.e. normalised DN values minus average DN value for the horizontal sites, against slope aspect and slope (Figure 4). In the NIR and MIR bands no consequent effect could be seen except for a slight over correction on the northern slopes. But in the visible bands, the residuals were more systematically ordered, revealing over correction on both northern and southern slopes. Figure 3b also show that in the red band the residuals were higher for sites with steeper slopes. The same can not be seen in the NIR band (Figure 3d).

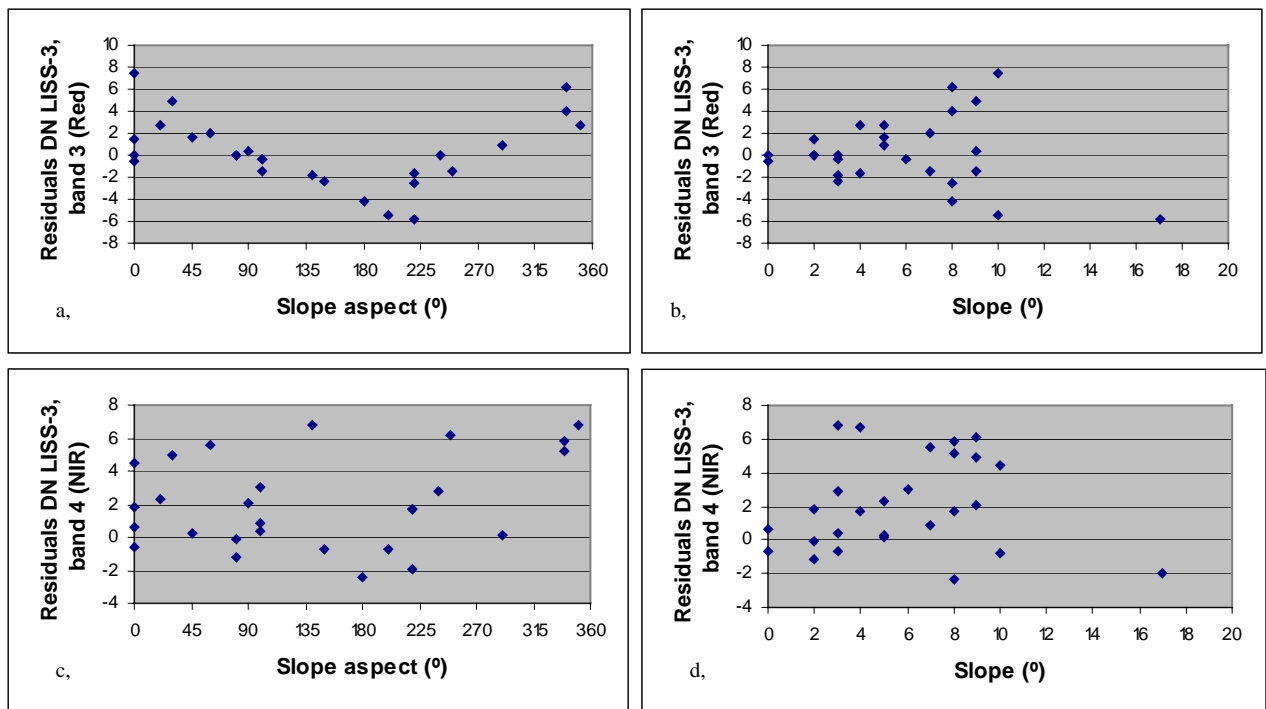


Figure 4: Topographic residuals (corrected DN values minus average DN value for horizontal sites) versus aspect and slope. Residuals in the red band versus aspect (a) and slope (b). Residuals in the NIR band versus aspect (c) and slope (d).

In Ekstrand (1993) residuals of estimated versus observed needle loss were plotted against slope. Although this is not fully comparable to the present case, it is interesting to see that the residuals in that study were larger on near horizontal than on steep slopes. The author explained this by the possibility that it is more difficult to measure aspect on near horizontal slopes, and that this may introduce larger errors in these sites.

It is important to bear in mind that the topographic residuals may be caused not only by a faulty correction, but also by variations in defoliation level and species composition. Perhaps also by variations in other parameters such as age, density and atmospheric aerosols. However, residuals remaining due to other factors than an unsuccessful correction would be randomly scattered, unless the factor causing the residuals is biased for certain aspects or slopes. Despite the somewhat over corrected data the results from the correlation analysis (section 3.2) proved that the topographic normalisation was successful.

3.1.2. Normalisation for species composition

Figure 5 show the spectral effect of a varying deciduous component on Landsat TM 4 and the LISS-3 bands.

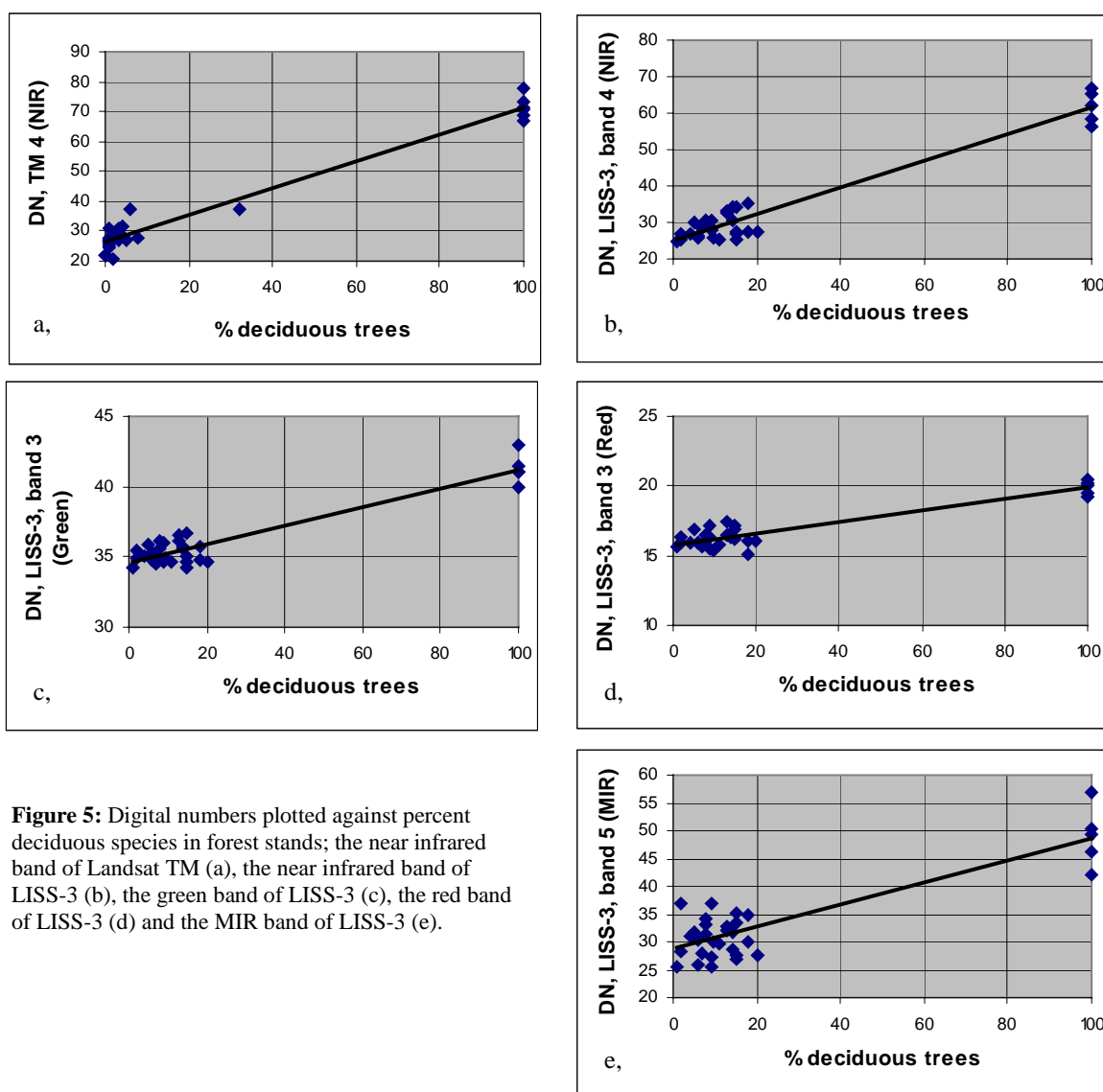


Figure 5: Digital numbers plotted against percent deciduous species in forest stands; the near infrared band of Landsat TM (a), the near infrared band of LISS-3 (b), the green band of LISS-3 (c), the red band of LISS-3 (d) and the MIR band of LISS-3 (e).

It is difficult to say anything about Figure 5 since no stand with a deciduous content within the range of 20 and 100 percent exists. In the NIR bands a correlation can clearly be seen though, but whether it is a linear or non-linear relationship is impossible to say. In the study where the original correction constants were developed (Ekstrand, 1993), a high correlation was found between percent deciduous trees and the NIR band, a lower correlation with the MIR band, and principally no relation with the visible bands. A similar result was obtained by Leckie (1987).

Although the spectral effect of an increasing deciduous component in the visible bands (Figure 4e) does not appear to be less than the effect in the MIR band, it is not very strong and no correction for species content was attempted for data from these bands. No study of Swedish forests has revealed a good correlation between needle loss and data from visible wavelengths. The correction was hence concentrated on data from the infrared bands.

While DN values for stands with different deciduous species content ranged from 20 to approximately 70 in the NIR band of TM, they ranged from approximately 25 to 60 in the LISS-3 NIR band (Figure 5). Corresponding values for the MIR band of LISS-3 were 28 to 50. A major reason why the range in LISS-3 NIR data was narrower than in the TM NIR data, was thought to be the difference in sun elevation. Whereas the TM scene was captured in early September, at a sun elevation of 33 degrees, the LISS data was registered at an elevation of 26 degrees in the end of September. Accordingly, correction coefficients were determined by calculating the ratio between the sun elevations of the two data sets, and multiply the original coefficients developed for TM NIR data with the ratio. The resulting coefficients are shown in Table 9.

Table 9: Correction coefficients for pine and deciduous components.

	Correction coefficient, Pine (DN)	Correction coefficient, Deciduous (DN)
LISS-3, 4, NIR	0,04	0,1
LISS-3, 5, MIR	0,02	0,06

It may seem strange that the correction coefficients do not reflect the slopes of the regressions in Figure 4b,e. The reason for this is may be that the relation between deciduous content in a spruce stand and satellite-registered radiance is not linear.

Maximum reduction of DN:s due to normalisation for species composition was 2 DN. The effect of the correction for species composition on radiance values is hence less than the correction for topography. No reference stand was composed of 100 percent spruce, and it was not possible to evaluate the correction by calculating residuals, i.e. corrected values subtracted by the value from 100 percent spruce stands. However, the results from the correlation analysis (section 3.2.) indicated that the species correction failed.

3.2. Correlation between spruce defoliation and LISS-3 data

The NIR band alone appears to be best correlated with defoliation (Table 10, Figure 6). This is in accordance with a number of studies (Brockhaus et al., 1992; Ekstrand, 1994; Ekstrand, 1998; Koch et al., 1990) although other authors have found highest correlation with MIR data and indices involving both NIR and MIR, or red, data (see section 1.2.). With the low resolution of the LISS-3 MIR channel in mind the low correlations with the MIR-band and indices involving the MIR-band, is not a surprise.

In previous studies where similar correction procedures as in the present study were employed, the correlation between defoliation and the NIR band of Landsat TM reached -0,80 (the same study area) and - 0,81 (south-west of Sweden) (Ekstrand, 1998). Brockhaus et al. (1992) studied defoliation in spruce-fir dominated forests of North Carolina. They found a correlation of - 0,81 with TM 4 (NIR) and - 0,74 with SPOT HRV 3 (NIR). When data was normalised for elevation the correlations increased to -0,93 and -0,89 respectively.

The correlation coefficients in this study were significantly higher for corrected than non-corrected data in all bands. This clearly shows the importance of correcting data for topographic effects. The correction for species composition did not affect the correlation coefficient particularly. It even resulted in a minor decline of the correlation, indicating that the normalisation procedure did not succeed in correcting for species composition. A correction employing larger correction constants were tested, but did not result in higher correlations. As have previously been discussed, the correlation between the content of pine and deciduous trees in a spruce stand and reflectance may be non-linear. There is a need for a thorough investigation of the effect of species composition on IRS data. Correction coefficients developed specifically for IRS data would probably yield a better result.

Table 10: Correlation between spruce defoliation and LISS-3 spectral bands and ratios.

Spectral band or ratio	Correlation coefficient, r raw data	Correlation coefficient, r corrected data ¹	Correlation coefficient, r corrected data ²
band 2 (green)	0,14	-0,52	-0,52
band 3 (red)	0,25	-0,41	-0,41
band 4 (NIR)	-0,19	-0,83	-0,82
band 5 (MIR)	0,006	-0,33	-0,31
Bands 5/4		0,29	0,31
Bands 4/3		0,33	0,33
NDVI (b4-b3/b4+b3)		0,42	0,42

¹ Normalised for terrain effects only.

² Normalised for terrain effects and for pine and deciduous components.

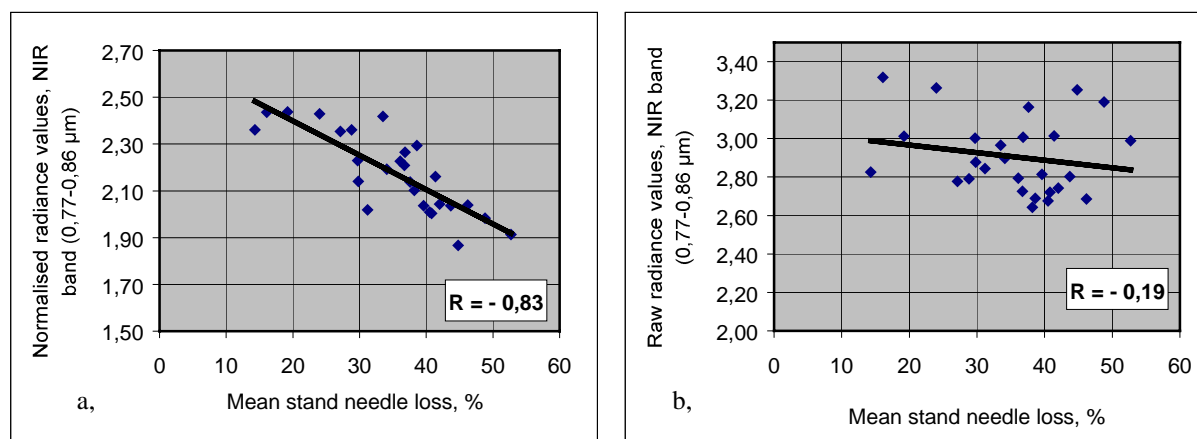


Figure 6: The relationship between IRS-1C LISS-3 band 3 (near-infrared) and spruce defoliation in 28 training stands of 1 hectare size; data corrected for atmospheric effects and normalised for topography and species composition (a), raw data (b).

Throughout this study the correlation coefficient was employed to describe the relationship between two variables. Its ability to measure the strength of the relations can of course be discussed, but this is beyond the scope of this report.

3.3. Defoliation assessment algorithm and verification

The resulting assessment algorithm was based on the regression line for the NIR band presented in Figure 6a (Equation 11).

$$D = 163,06 - 45,546 \cdot L(\text{NIR})_{\text{corr}}$$

Equation 11

D = Defoliation (%)

$L(\text{NIR})_{\text{corr}}$ = Near infrared radiance normalised for topography and species composition ($\text{mWcm}^{-2}\text{sr}^{-1}\mu\text{m}^{-1}$)

Despite the fact that there were no sites with less than 25 percent mean needle loss in the verification set, the correlation between predicted and observed defoliation was 0,70 (Figure 7). Root mean square was 3,1 percent needle loss.

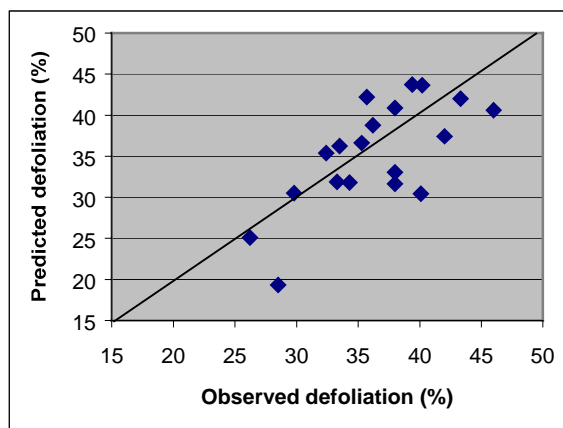


Figure 7: Observed versus predicted defoliation in reference sites used for evaluation.

The majority of stands in Västernorrland have a mean needle loss in the range of 20 to 45 percent. Only three sites had lower values, but these were needed for the correlation analysis. A fact that may affect the prediction of defoliation in the verification sites is that slope and aspect were estimated from air photos and not in field. However, in an operational context slope and aspect would be derived from a digital elevation model, which presumably would yield a slightly lower correlation.

3.4. IRS LISS-3 versus Landsat TM

This study indicates that the performance of IRS LISS-3 for defoliation studies of Norway spruce (*Picea abies*) is comparable to that of Landsat TM. It could very well be used as an alternative to TM data, which would significantly increase the possibility to obtain cloud free satellite data.

However, there are a couple of reasons why data from the TM sensor may be preferred. One is that the sensor has been in use for a quite long time and much research has been made on its performance, e.g. the calibration of the sensor is better known and studies of its decay with time has been performed. Another reason is that the radiometric performance of TM appears to be better. It registers the electromagnetic radiation in an 8-bit resolution while LISS-3 registers in 7 bits. Channel offsets are also higher in LISS-3 than in TM (Table 5) which means that the dynamic range of the sensor is lower than for Landsat TM. This may be important in defoliation studies where relatively low values of radiance are considered. However, it may also be that the sensitivity of LISS-3 is concentrated on the most interesting radiance interval so that the lower dynamic range does not affect the defoliation assessment at all.

3.5. Error sources

3.5.1. Delineation of reference sites in the satellite scene.

Delineation of reference sites in the satellite scene was performed manually. Choosing which pixels should be included and which should not, is a critical and subjective step of the study.

An alternative would have been to calculate map co-ordinates for the sites from the aerial photographs, and then add them to the satellite in an overlay process. However the total Root Mean Square Error, RMSE, for the geometric correction was 10,3 m., i.e. less than one pixel. Maximum RMSE for a single GCP was 15 m. Better accuracy is rarely achieved. Still the geometric displacement may locally be as high as one pixel, and an arbitrary displacement of one pixel could have detrimental effects on the defoliation assessments.

3.5.2. Correction for varying forest stand parameters

Correction for pine and deciduous components was achieved using correction coefficients empirically derived from another data set. Although the coefficients were modified based on the difference in sun elevation between the two data sets, a proper procedure would have been to develop completely new coefficients from the IRS data set. This however required a large number of stands with varying degrees of pine and deciduous components but very narrow ranges of age, density and defoliation, and such a data set was not available.

Age and density were attended by excluding stands older than 70 years as well as sparse stands from the study. This was performed by visual inspection of air photos. The resolution of the air photos was high and only minor errors are likely to have been introduced. Forest younger than 70 years is rarely affected by defoliation in the region, and defoliation assessments of these stands are not really urgent. Stands with low densities may occur despite that most forests in Sweden are used in production and are intensively managed. Even though they do not occur very frequently, it would be good to be able to assess defoliation also in stands with low densities. While in this study only selected stands were studied, an operational context requires a more automatic approach to obtain information of age and density of the forest. Ekstrand (1996, 1998) has integrated digital forest maps with satellite data to obtain information on forest parameters. But digital forest maps do not exist over all forests, and are time and cost consuming to produce. It will thus be interesting to see which potential the forthcoming high-resolution satellite data has for classification of forest parameters such as age, density (and gaps) and species.

3.5.3. Correction for topography

The topographic normalisation algorithm employed in the study was also originally developed for Landsat TM data. A procedure optimised for LISS-3 should be produced when a sufficiently extensive reference data set is available.

3.5.4. Errors in reference data

Ekstrand (1991) examined the accuracy of air photo interpreted estimations of defoliation (on a scale of 1:6000). He found that 71 % of 100 trees were classified into the correct class. However, when comparing the mean values of the interpreted defoliation with the mean value of the field assessment, they were very similar; 32,5 versus 29,9 percent.

The accuracy of species interpretation in 1:6000 air photos, is approximately 95 percent for pine trees and 100 percent for deciduous trees (Ekstrand 1993).

3.5.5. Radiometric correction

The absolute values of radiance presented in the study should be considered with caution. Conversion of digital numbers to at satellite radiance was based on calibration data from the contractor. The author does not know exactly how these calibration coefficients were produced, but according to EuroMap (Zahn, C. personal communication, 1998) no post-launch calibration campaign has been performed. This means that no account has been taken to the decay of the sensor with time. Moran et al. (1995) have studied the decreasing response with time for the Landsat TM and SPOT HRV sensors. They found a sharp decrease in response shortly after launch in both sensors.

Correcting for atmospheric effects with a dark object subtraction is a rather rough approach. A proper set of input to the widely used 6S software (Second Simulation of Satellite Signal in the Solar Spectrum) is generally thought to give a better correction for atmospheric disturbances (Alm, personal communication, 1998). However, with the assumption of a homogeneous atmosphere the atmospheric correction does not influence correlations and regressions based on single bands, but only ratios and spectral profiles. The assumption of a homogeneous atmosphere is rarely valid though, but data on aerosol and water content with a sufficient spatial resolution is not available in Sweden.

4. Conclusion

There is a relatively strong correlation between the near infrared band of IRS-1C LISS-3 and Norway spruce defoliation (*Picea abies*) in the county of Västernorrland, Sweden. This is in accordance with earlier results from the same area where Landsat TM data were used. IRS LISS-3 data may very well be used as an alternative to Landsat TM for defoliation estimations, although the results would probably not be significantly improved.

The normalisation for topography improved the correlations between air photo interpreted defoliation and satellite data in all channels. In the near infrared domain the correlation coefficient increased from -0,19 to -0,82 after normalisation. However, in the visible wavelength bands the normalisation resulted in over corrected values. Radiance was increased too much on north facing slopes and reduced too much on south facing slopes. This effect appeared to be more pronounced for steeper than near horizontal slopes. The same tendency could not be seen in data from the near and middle infrared domains, where the residuals were evenly distributed among aspects and slope gradients. Nevertheless the correction must be considered adequate bearing in mind the marked increase of the correlation coefficient between all bands of the satellite data and needle loss.

Correction for species composition in the forest sites did not improve the correlations. In some cases the correction coefficients even decreased. The procedures employed for both species and topography correction were initially developed for Landsat TM data. A thorough investigation of the effect of topography and species composition, particularly the latter, on LISS-3 data is desired.

Despite the unsuccessful species correction, and the fact that no stand with less mean defoliation than 25 percent were present in the verification set, the correlation coefficient between predicted and observed needle loss was 0,70, and mean needle loss error was 3,1 percent.

References

- Alm, G., 1998. Personal communication. Department of Physical geography, Stockholm university, Sweden.
- Ardö, J., 1998. *Remote sensing of forest decline in the Czech Republic*. Ph.D. thesis, Lund university, Lund, Sweden.
- Berghäll, S., Wijk, S., Wulff, S. and Söderberg, U. 1995. Skogsskador i Sverige 1994. *Resultat av skogsskadebevakning från riksskogstaxeringen och skogsvårdsorganisationens observationsytor*. Skogsstyrelsen, Rapport 1995:4, Skogsstyrelsens förlag, Jönköping, Sweden.
- Brockhaus, J.A., Khorram, S., Bruck, R.I., Campbell, M.V. and Stallings, C., 1992. A comparison of Landsat TM and SPOT HRV data for use in the development of forest defoliation models. *International Journal of Remote Sensing* 13(16): 3235-3240.
- Bukata, R. R., Bruton, J.E. and Jerome, J.H., 1983. Use of chromaticity in remote measurements of water quality, *Remote Sensing Environment* 13:161-177.
- Chavez, P.S., Jr., 1988. An improved dark-object subtraction technique for atmospheric scattering correction of multispectral data. *Remote Sensing Environment* 24:459-479.
- Civco, D.L., 1989. Topographic normalization of Landsat Thematic Mapper digital imagery. *Photogrammetric Engineering and Remote Sensing* 55(9): 1303-1309.
- Colwell, J.E., 1974. Vegetation canopy reflectance. *Remote Sensing Environment* 3:175-183.
- Deering, D.W. Middleton, E.M. and Eck, T.F., 1994. Reflectance anisotropy for spruce-hemlock forest canopy. *Remote Sensing Environment* 47:242-260.
- Ekstrand, S., 1991. *Effekter av luftföroreningar från vägtrafik på närliggande skog. Flygbildsbedömning av kronutglesning på gran*. IVL-report B-1016, Stockholm, Sweden.
- Ekstrand, S., 1993. *Assessment of forest damage with Landsat TM, elevation models and digital forest maps*. Ph.D. thesis, Royal Institute of Technology, Stockholm, Sweden.
- Ekstrand, S., 1994. Assessment of forest damage with Landsat TM: Correction for varying forest stand characteristics. *Remote Sensing Environment* 47:291-302.
- Ekstrand, S., 1996. Landsat TM based forest damage assessment Correction for topographic effects. *Photogrammetric Engineering and Remote Sensing* 62(2), 151-161.
- Ekstrand, S. and Hansen, C., 1998. *Pilot study on the use of satellite data for regional forest condition surveys*. Proj. no. 96.60.SW.004.0. IVL-report B-1281, Stockholm, Sweden.
- Franklin, J., 1986. Thematic Mapper analysis of coniferous forest structure and composition. *International Journal of Remote Sensing* 7:1287-1301.
- Hammond, R. and McCullough, P.S., 1978. *Quantitative techniques in geography: an introduction*, 2nd ed. Oxford University Press, 364 pp.
- Heikkilä, J. 1998. *Monitoring boreal coniferous forest health in Finland using the reference sample plot method with multisource and multitemporal data*. Fil. Lic. Thesis, University of Joensuu, Finland.
- Häusler, T., 1991. *Waldschadenkartierung in Fichtenrevieren durch Auswertung von Satellitenaufnahmen und raumbezogenen Zusatzdaten*, Dissertation Uni Freiburg, Germany. [Mapping forest damages in Norway spruce areas by analysing satellite images and ancillary data].
- Hällgren, J.-E., 1995. Skogstillväxt – klimat. In: *Kritiska faktorer för skogsträdens tillväxt och vitalitet, Konferens den 29 mars 1995 anordnad av stiftelsen Svensk växtnäringforskning.*, Agerlid, G., (ed). Kungl. Skogs- och lantbruksakademien, Sweden.
- Kalyanaraman, S., Rajangam, R.K. and Rattan, R., 1995. Indian remote sensing spacecraft – 1C/1D. *International Journal of Remote Sensing* 16:791-799.
- Kaufman, Y.J. and Tanré, D., 1996. Strategy for direct and indirect methods for correcting the aerosol effect on remote sensing: from AVHRR to EOS-MODIS. *Remote Sensing Environment* 55:65-79.

- Kawata, Y., Ueno, S. and Kusaka, T., 1988. Radiometric correction for atmospheric and topographic effects on Landsat MSS images. *International Journal of Remote Sensing* 9(4):729-748.
- Kleman, J., 1986. The spectral reflectance of stands of Norway spruce and Scotch pine, measured from a helicopter. *Remote Sensing of Environment* 20:253-256.
- Koch, B., Ammer, U., Schneider, T. and Wittmeier, H., 1990. Spectroradiometer measurements in the laboratory and in the field to analyse the influence of different damage symptoms on the reflection spectra of forest trees. *International Journal of Remote Sensing* 11(7), 1145-1163.
- Kowalik, W.S., Lyon, R.J.P and Switzer, P., 1983. The effects of additive radiance terms on ratios of Landsat data. *Photogrammetric Engineering and Remote Sensing* 49(5):659-669.
- Kriebel, K.T., 1976. On the variability of reflected radiation field due to differing, distributions of the irradiation. *Remote Sensing of Environment* 4:257-264.
- Lambert, N.A., Ardö, J., Rock, B.N. and Vogelmann, J.E., 1995. Spectral characterization and regression-based classification of forest damage in Norway spruce stands in the Czech Republic using Landsat Thematic Mapper data. *International Journal of Remote Sensing* 16(7), 1261-1287.
- Leckie, D.G., 1987. Factors affecting defoliation assessment using airborne multispectral scanner data. *Photogrammetric Engineering and Remote Sensing* 53(12): 1665-1674.
- Leckie, D.G., Teillet, P.M., Fedosejevs, G. and Ostaff, D.P., 1988. Reflectance characteristics of cumulative defoliation of balsam fir. *Canadian Journal of Forest Research* 18:1008-1016.
- Lillesand, T.M. and Kiefer, R.W., 1994. *Remote sensing and image interpretation*, 3rd ed, Wiley and sons, USA, 729 pp.
- Markham, B.L. and Barker, J.L., 1987. Thematic Mapper bandpass solar exoatmospheric irradiances. *International Journal of Remote Sensing* 8(3), 517-523.
- Meyer, P., Itten, K.I., Kellenberger, T. Sandmeier, S. and Sandmeier, R., 1993. Radiometric corrections of topographically induced effects on Landsat TM data in an alpine environment. *ISPRS Journal of Photogrammetry and Remote Sensing* 48(4):17-28.
- Minnaert, M., 1941. The reciprocity principle in lunar photometry. *Astrophysical Journal* 93:403-410.
- Moran, M.S., Jackson, R.D., Clarke, T.R., Qi, J., Cabot, F., Thome, K.J. and Markham, B.L., 1995. Reflectance factor retrieval from Landsat TM and SPOT HRV data for bright and dark targets. *Remote Sensing of Environment* 52:218-230.
- National Forest Inventory, 1998. *Skogsdata*. Excel data on forest taxations 1992-1996, Institutionen för skoglig resurshushållning och geomatik, SLU, Umeå, Sweden.
- Nihlgård, B., 1996. Skogsskadornas mångfaldiga bakgrund. *Skog och forskning* 3:6-12.
- Rock, B., Hoshizaki, T. and Miller, J.R., 1988. Comparison of in-situ and airborne spectral measurement of the blue shift associated with forest damage. *Remote Sensing of Environment* 24:109-127.
- Schulze, E-D., 1989. Air pollution and forest decline in a spruce (*Picea abies*) forest. *Science*, 244: 776-783.
- Smith, J.A., Lin, T.L. and Rasnson, K.J. 1980. The Lambertian assumption and Landsat data. *Photogrammetric Engineering and Remote Sensing* 46(9): 1183-1189.
- Swain, P. H. and Davis, S.M. (eds), 1978. *The quantitative approach*, Chapt. 5, McGraw-Hill, New York, .
- Teillet, P.M., Guindon, B. and Goodenough, D.G., 1982. On the slope-aspect correction of multispectral scanner data. *Canadian Journal of Remote Sensing* 8(2):84-106.
- Thomson, A.G. and Jones, C., 1990. Effects of topography on radiance from upland vegetation in North Wales. *International Journal of Remote Sensing* 11(5):829-840.
- Vogelmann, J.E. and Rock, B.N., 1988. Assessing forest damage in high-elevation coniferous forests in Vermont and New Hampshire using Thematic Mapper data. *Remote Sensing of Environment* 24:227-246.
- Vogelmann, J.E., 1990, Comparison between two vegetation indices for measuring different types of forest damage in the north-eastern United States. *International Journal of Remote Sensing* 12:2281-2297.

Wastenson, L., Alm, G., Kleman, J. and Wastenson, B., 1987. Swedish experiences on forest damage inventory by remote sensing methods. *International Journal of Aerial and Space Imaging, Remote sensing and Integrated Geographical Systems* 1(1):43-52.

Wolfe, W.L. and Zissis, G.J., 1989. *The infrared handbook*. The infrared information analysis center, Environmental research institute of Michigan.

Wulff, S. and Löfgren, O., 1998. *Instruktion för fältarbetet vid riksskogstaxeringens skogsskadeinventering år 1998*. Institutionen för skoglig resurshushållning och geomatik, Umeå.

Yugui, Z., 1989. *Normalization of Landsat TM imagery by atmospheric correction for forest scenes in Sweden*. Research Report, Remote Sensing Laboratory, Swedish University of Agriculture Sciences, Umeå.

Zahn, C., 1998. Personal communication. Euromap, Germany.



IVL Svenska Miljöinstitutet AB

Box 210 60, SE-100 31 Stockholm
Hälsingegatan 43, Stockholm
Tel: +46 8 598 563 00
Fax: +46 8 598 563 90

www.ivl.se

IVL Swedish Environmental Research Institute Ltd

Box 470 86, SE-402 58 Göteborg
Dagjämningsgatan 1, Göteborg
Tel: +46 31 725 62 00
Fax: +46 31 725 62 90

Aneboda, SE-360 30 Lammhult
Aneboda, Lammhult
Tel: +46 472 26 20 75
Fax: +46 472 26 20 04